

## Supplementary Information for

An unbiased approach elucidates variation in (S)-(+)-linalool, a context-specific mediator of a tri-trophic interaction in wild tobacco

Jun He, Richard A. Fandino, Rayko Halitschke, Katrin Luck, Tobias G. Köllner, Mark H. Murdock, Rishav Ray, Klaus Gase, Markus Knaden, Ian T. Baldwin, Meredith C. Schuman

Ian T. Baldwin, Meredith C. Schuman  
Email: [baldwin@ice.mpg.de](mailto:baldwin@ice.mpg.de), [meredith.schuman@geo.uzh.ch](mailto:meredith.schuman@geo.uzh.ch)

### **This PDF file includes:**

Supplementary text  
Figs. S1 to S12  
Tables S1 to S3  
References for SI reference citations

### **Other supplementary materials for this manuscript include the following:**

Datasets S1 to S3

## Supplementary Information Text

### Plant materials and growth conditions

The two *N. attenuata* natural accessions AZ and UT were collected from populations near Flagstaff, Arizona (1) and the DI Ranch, T40S R19W section 9 of Utah (2), and inbred for 22 (Arizona) or 30 (Utah) generations in the glasshouse. The generation of the advanced intercross-recombinant inbred line (AI-RIL) population was previously described (3); generation F11 was used for glasshouse experiments and seed from these plants, F12, in the field experiment. The other *N. attenuata* natural accessions were collected in the southwestern United States from the locations shown in Fig 2I. The full-length cDNAs of *CbLIS* (4) and *ObLIS* (5) were cloned from plasmids kindly provided by E. Pichersky and transferred into the pSOL9 plasmid (6). *Agrobacterium tumefaciens* (strain LBA 4044)-mediated transformation proceeded as previously described (7). Multiple *N. attenuata* stable lines ectopically expressing *CbLIS* and *ObLIS* under control of the CaMV35 promoter were generated in both UT and AZ genotype backgrounds. Diploid transgenic lines were screened using flow cytometric analysis (8). Homozygous T2 plants of each line were identified using seedling resistance to hygromycin (6). Ectopic expression lines of *CbLIS* and *ObLIS*, and the RNAi silencing line of *irMPK4* (9) used in this study are listed in Table S2.

Seed germination followed the protocol by Krügel et al. (7). After 10 days, seedlings were transferred to small pots (TEKU JJP 3050 104 pots, Poepelmann GmbH & Co. KG, Lohne, Germany) in the glasshouse and then to 1 L pots 10 days later. For most assays, plants were grown with soil, fertilization and watering regimes as previously described, and grown under 19°C–35°C with a light period of 6:00-22:00 (supplemental lighting by Philips Sun-T Agro 400 W and 600 W sodium lights) and 55% humidity (7, 10). For the VIGS experiment, plants were grown with the same soil and fertilization regime in a climate chamber (22 °C; light period: 6:00 to 22:00, supplemental lighting by Philips Sun-T Agro 400 W and 600 W sodium lights; 65% relative humidity). For experiments in the field, seedlings were adapted to field conditions similarly to previous studies (11, 12) with the following changes: seedlings in closed boxes were kept in a shady location directly on the soil, and hardening-off was done by opening boxes and then reducing shade cover two days later. Seedlings with a rosette diameter of ca. 1.5-2.5 cm were transplanted in to a field plot at the Walnut Creek Center for Education and Research (34°55'17.8"N 112°50'42.2"W) located in Arizona. Plants were watered in the early morning and evening using a drip irrigation system until they had established, and then as needed. The planting arrangement in the field is described under “Predation assay” in the Materials and Methods section of the main text.

### Plant treatment and headspace sampling

RIL plants in the glasshouse were treated with wounding and *M. sexta* regurgitant to induce defense responses. Collection of regurgitant from caterpillars reared on *N. attenuata* UT WT plants, storage, and treatment was as previously described (13, 14). Briefly, the rosette-stem transition leaf (S0) or the first stem leaf (S1) (15) of elongated plants was wounded using a pattern wheel on each side of the midvein and 20 µL of regurgitant diluted 1:5 with distilled water were added to the wounds and gently rubbed in with a clean, gloved finger. Following treatment, the leaf was enclosed in a clean,

ventilated PET cup (ca. 650 mL) with two pieces of silicone laboratory tubing (ST, 1 mm i.d. x 1.8 mm o.d.; Carl Roth, catalog number: 9555.1; 5mm for each piece) to absorb plant volatiles and equilibrate with the headspace over 24 h (16, 17). Transgenic plants for screening were not elicited and the youngest rosette leaf was used for treatments and volatile sampling from elongating plants. Volatile sampling from VIGS plants followed the same protocol. For diurnal emission and light deprivation experiments using UT WT plants, volatiles were sampled during the night (22:00-6:00), and every 4h after that over the day. Light deprivation was applied by wrapping the collection cup with aluminum foil from 10:00-14:00. To assess diurnal emissions of linalool in transgenic plants, the headspace was sampled for three different periods: dusk (18:00-22:00), night (22:00-6:00), and day (6:00-14:00).

#### TD-GC-QMS analysis

One piece of ST was placed into a glass TD tube (Supelco, [www.sigmaaldrich.com](http://www.sigmaaldrich.com)) and analyzed on a quadrupole GC-MS-QP2010Ultra equipped with a TD-20 thermal desorption unit (Shimadzu). For linalool quantification in RILs, accessions and transgenic plants, as well as the relative quantification of other terpenoids (Figs. S8 and S9, Supplementary Datasets D2 and S3), a ZB-Wax plus GC column (Phenomenex, 30 m x 0.25 mm x 0.25  $\mu$ m) was used to analyze total linalool. Desorption and analysis were performed as previously described (16, 17). For enantiomer identification, a Cyclosil B column (Agilent, 30 m x 0.25 mm x 0.25  $\mu$ m) was used and the GC program was modified: the oven program started at 40 °C and after a 2 min hold, increased to 80°C at 40°C/min, then to 140 °C at 5 °C/min, then to 200°C at 40°C/min followed by a 1 min hold.

Peaks were integrated using the target and reference ions listed in Table S1 and compound identifications were based on comparison of spectra and retention indices against NIST libraries. The linalool spectrum and retention time was compared to pure standards [racemic linalool and (*R*)-(-)-linalool, Sigma-Aldrich].

#### QTL mapping

The genotyping of the AI-RIL population and linkage map were reported by Zhou, *et al.* (3). QTL mapping was performed using R package QTLRel (18) following the workflow previously described by Zhou *et al.* (3), based on the relative abundance of each compound in the 261 lines of the population.

#### Measuring transcript abundance of genes

The transcript abundance of *NaLIS*, *NaGPPS1*, *NaGPPS2* were measured using qPCR. For correlation between internal free linalool (see below) and transcript abundance, the youngest rosette leaf of an elongating plant was used for both volatile extraction and RNA extraction. Total RNA was isolated and genomic DNA was digested using the NucleoSpin® RNA Plant kit (MACHEREY-NAGEL) according to the manufacturer's protocol. About 1  $\mu$ g total RNA were reverse transcribed using the PrimeScript™ RT reagent Kit (TAKARA). The relative transcript abundance of the target genes was measured using qPCR with a MX3005P PCR cycler (Stratagene). Transcript abundance of *NaLIS* in the VIGS experiment was measured the same way

using similar leaves. The eukaryotic translation initiation factor 5A-3 (*IF5A3*) was used as reference for normalization. Primers used for qPCR are listed in Table S3.

#### Measurement of internal free linalool and glycosides

Internal free linalool was extracted from leaf tissue using ST pieces (17) following a protocol modified from van Pinxteren *et al.* (19) and Matsui *et al.* (20). Briefly, the youngest rosette leaf of an elongating plant was harvested, flash-frozen and ground in liquid N<sub>2</sub>. Distilled water saturated with CaCl<sub>2</sub> (0.8 ml) was added to ground tissue (~100 mg) in a 1.5 ml glass GC vial (Sigma-Aldrich) to inhibit enzyme activity. One piece of ST (1 mm i.d. x 1.8 mm o.d.; Carl Roth, catalog number: 9555.1; 5mm for each piece) was placed into the vial to extract volatiles from tissue.

Linalool conjugates were extracted and released following a protocol modified from Lucker *et al.* (21). Briefly, about 200 mg ground tissue (precise mass recorded) of the youngest rosette leaf of an elongating plant was extracted with 1 mL 80% MeOH. Extracts were dried completely under nitrogen gas in a 1.5 mL GC vial. Then 100 µL citric acid/phosphate buffer (pH 5.2) and 100 µL almond β-glucosidase (Sigma) solution (6 units) were added to the sample along with one piece of ST and incubated overnight at 37 °C. ST pieces with collected internal volatiles were washed in MilliQ water and dried briefly under nitrogen gas before measurements.

#### Analysis of *NaLIS* allelic variants and transcript abundance in 26 accessions

The genomic sequence of *NaLIS*-UT was extracted from the genome data in the *Nicotiana attenuata* Data Hub [<http://nadh.ice.mpg.de>, (22)]. Scaffolds containing the *NaLIS*-AZ sequence in the AZ genome were identified using *NaLIS*-UT as query. Genomic and transcript sequences of *NaLIS*-AZ and *NaLIS*-UT were aligned using megablast (<https://blast.ncbi.nlm.nih.gov>). The 3' end of the *NaLIS* transcript alleles in ten accessions were amplified using primers listed in Table S3.

The entire chromosome VIII was extracted from the reference genome (23) and the region of interest was identified within it. The nucleotide sequence from that region was aligned pairwise with the putative AZ sequence. The pairwise alignment was merged using a python script to create an augmented reference sequence and was then indexed using BWA (24). The whole genome sequences of 26 accessions were then aligned to this augmented reference using bwa mem aligner (24). Additionally, MAKER2 (25) in conjunction with AUGUSTUS (26), SNAP (27), and Genemark (28) used to predict de novo gene model within the augmented sequence. The mRNA sequence was extracted from the gene model and RNA-Seq data from 26 wound elicited leaf samples were aligned and quantified using kallisto (29) on the modified transcriptome containing the “augmented” gene. Finally, to obtain the consensus sequence with respect to the reference, genome coverage was calculated at each base in that region using bedtools *genomecov* function (30) and filtered where coverage was greater than 1. The contiguous bases were then merged using the bedtools *merge* function to identify the deleted regions. These regions were then visualized in IGV (31) to visually confirm the deletions for each accession.

#### Heterologous expression of *NaLIS* in *Escherichia coli* and extraction of recombinant protein

The full-length ORF of *NaLIS* as well as the N-terminal truncated ORF lacking the region encoding a putative signal peptide (nucleotides 1-87) were amplified from cDNA made from leaves of AZ and UT plants separately with primers listed in Table S3. Purified PCR fragments were cloned into the bacterial expression vector pET200 (Invitrogen). The procedure of expression and protein extraction followed the previous description (3).

#### Analysis of recombinant NaLIS

To determine the catalytic activity of NaLIS, enzyme assays containing 40  $\mu$ L of the bacterial protein extract and 60  $\mu$ L assay buffer with 40  $\mu$ M GPP, (*E,E*)-FPP, or (*E,E,E*)-GGPP and 10 mM MgCl<sub>2</sub>, were performed in Teflon-sealed screw-capped 1.5 mL GC glass vials. Assays were overlaid with 100  $\mu$ L hexane, incubated for 120 min at 25°C, and vortexed for 1 min to extract enzyme products from the aqueous phase. The hexane phase was then collected and analyzed using GC-MS. As a negative control, raw protein extracts from *E. coli* expressing the empty vector pET200 were incubated with the substrates GPP, (*E,E*)-FPP, and (*E,E,E*)-GGPP, respectively, as described above. No TPS enzyme activity was observed in negative controls.

TPS enzyme products were analyzed on an Agilent 6890 Series gas chromatograph coupled to an Agilent 5973 quadrupole mass selective detector. Measurements using a DB-5MS column (Agilent, Santa Clara, USA, 30 m x 0.25 mm x 0.25  $\mu$ m) followed the procedure previously described (3). Product identification was done using authentic standards (linalool, nerolidol, Sigma-Aldrich) or the WILEY mass spectra library (geranylinalool).

#### VIGS of NaLIS

Two hundred bp of the coding sequence of *NaLIS* were amplified using PCR with primers given in Table S3 and transferred into the PTV vector for VIGS. The VIGS followed the procedures described by Galis, *et al.* (32). Silencing efficiency was tested by measuring transcript abundance using qPCR, and headspace volatiles were sampled, as described above.

#### T-DNA copy number and integrity determination using NanoString's nCounter® Technology

Procedures are described in the main text. Here, we provide details of the 12 code probe set.

For the nCounter analysis, a 12 code probe set (sequences in Supplementary Dataset S1) was designed from 12 chosen target regions, which comprised 3 calibrator genes that occur as a single copy in the genome of *N. attenuata* [*AOC\_2*: allene oxide cyclase (GenBank LOC109240002); *S-RNase-2\_1*: ribonuclease S-7-like (GenBank LOC109235079); *sulfite\_2*: sulfite reductase 1 (GenBank LOC109217753)], and 9 functional regions present on the pNAT (33), pRESC (34-36), pSOL (33), and pPOP6 (37) binary vectors used in our group for the transformation of *N. attenuata*. These target sequences are indicative of complete T-DNA insertions (TNOS+LB\_1: terminator of the nopaline synthase gene; *hptII\_3*: hygromycin phosphotransferase gene; PNOS\_1: promoter of the nopaline synthase gene; P35S\_1: cauliflower mosaic virus 35S promoter; T35S\_1: cauliflower mosaic virus 35S terminator; *sat-1\_1*: streptothricin

acetyltransferase; *nptIII\_1*: neomycin phosphotransferase II gene) or T-DNA overreads (pVS1\_3: pVS1 vector backbone; *nptIII\_3*: neomycin phosphotransferase III gene) of the specific transformation vectors. The oligonucleotides were designed by NanoString (Seattle, WA, USA) and synthesized by IDT (Integrated DNA technologies). The location of the target sequences on the binary plant transformation vectors is indicated in Fig. S10B.

#### *Manduca sexta* rearing, pupation, mating

*M. sexta* used in this study were from an in-house colony. Eggs were collected from *D. wrightii* plants placed in an oviposition cage (2m x 1.5m x 1m) with mated moths, inside of a climate chamber (24 °C, light period: 0:00 to 13:00, relative humidity: 70%). In the same chamber, eggs were hatched in a small plastic box (8cm x 5cm x 4cm) with small holes on the lid and reared there with artificial diet (38) until the second instar. Then the caterpillars were transferred into a larger plastic box (30cm x 20cm x 20cm) with a plastic shelf at the bottom and dirty boxes were regularly replaced with clean boxes. When the caterpillars were ready to pupate, they were individually transferred into holes in a wood block and covered by wood panels. Pupae were removed about two weeks later. For oviposition assays in the wind tunnel or tent, male and female pupae were separated and placed into paper bags in cages (1 m x 0.4 m x 0.4 m). The cages were placed either in the climate chamber (wind tunnel), or at the Isserstedt glasshouse where the tent was located (tent). Two days after emergence, two males and one female were put into a cage (30 cm x 30 cm x 30 cm) for overnight mating. Mated females were then used for assays on the following day. For the oviposition assay in the climate chamber, approximately equal numbers of male and female pupae were regularly placed on a paper shelf with holes in an open paper box in the chamber. Moths emerged from these pupae were allowed to mate freely and kept in the chamber during the experiments.

#### Oviposition assay in wind tunnel, oviposition chamber and tent

The oviposition behaviors of newly mated *M. sexta* female adults were observed in the wind tunnel of the MPICE. The wind tunnel (240 cm × 90 cm × 90 cm) was set to the following conditions: 25 °C and 75% relative humidity, a wind speed of 0.4 m/s and a light level of 0.5 lux (39). Plants and moths were placed into separate chambers having the same conditions as the wind tunnel one hour before the assay (movement to chambers at 13:00, assay at 14:00). Then a pair of plants was placed upwind in the wind tunnel at a precise location such that the stems of plants (about 50 cm high) were 42 cm from each other, 24 cm from each side and 30 cm from the upwind wall of the wind tunnel. A single mated moth in a black mesh cage (15 cm × Ø13 cm) was placed onto a platform at the downwind end of the tunnel (45 cm from the sides, 10 cm from the downwind end and 30 cm from the floor). Then the top and side parts of the cage were removed and the moth was exposed to wind and plant odors. The wings of the moth were lightly touched by fingers until the moth started beating its wings. The moth was allowed to fly in the wind tunnel until it touched plants 10 times. The identity of the plant touched each time was immediately recorded. After 10 touches, the moth was removed from the wind tunnel. Then the plants were removed and the number of eggs on each plant was counted and recorded. As a backup, a video camera (Logitech C615, USA, infrared filter removed) recorded the wind tunnel from the release of the moth to the 10 touches of plants. For

every comparison between two genotypes, 20 pairs of plants and 20 moths were assayed. The relative placement of genotypes was switched for each moth.

Overnight oviposition of *M. sexta* adults was assayed in an oviposition chamber (1.4 x 1.5 x 2.0 m, light period: 6:00 to 22:00), where a small colony of *M. sexta* moths containing about 3-5 females and a similar number of males of different ages were continuously kept and regularly renewed. Two genotypes (4 plants each) were placed into the chamber. Plants of the same genotype were positioned in one row and the two rows of different genotypes were 1.5 m apart. The plants were kept there overnight (20:00-8:00) with moths, and then plants were removed and the eggs on each plant were carefully collected with fingers in gloves and counted. In total, 20 plants were assayed for each comparison of two different genotypes. Relative places of the rows of different genotypes in the chamber were switched every day.

Oviposition of *M. sexta* on multiple plants was further assayed in a tent located in Isserstedt, Jena, Germany, in July, 2018. The tent (24 m × 8 m × 4 m, Amiran, Kenya, [www.amirankenya.com](http://www.amirankenya.com)) is located outdoors and covered with mesh at the sides and front, permitting air exchange (11). The ground of the tent lacked vegetation (mostly grass) which was removed before experiments. Ten plants of each of six genotypes tested were placed in the tent, forming a population of 60 plants with each plant positioned 1.5 m apart. The plants were distributed in ten blocks each containing all six lines, and the positions of different lines were randomized within each block and randomly switched within the block every day during the assay period. Each day, a single mated *M. sexta* female moth was released into the tent at 16:00 and kept there overnight. The moth was removed at 11:00 on the following day and eggs were carefully collected from each plant without damaging the leaves. The number of eggs from each plant was counted. Different moths (days) were used as replicates. In total, 16 moths were assayed and 12 moths which laid a reasonable amount (> 20) of viable eggs were used for statistical analysis.

#### Metabolite extraction from plant leaves and *M. sexta* frass, and LC-MS analysis

One hundred mg ground leaf material or 30 mg *M. sexta* frass was extracted in 1 mL 80% methanol in a 1.5 mL Eppendorf tube. Two steel balls were added to the solution with leaf or frass material and tubes were shaken twice at 1200 strokes/min for 1 min using a Geno/Grinder 200 (SPEX SPEX SamplePrep, <http://www.spexsampleprep.com/>). Tubes were centrifuged at 16 000 g for 20 min at 4 °C and the supernatant was transferred to a new tube and re-centrifuged. The supernatant (500 µL) was then transferred to a glass vial with a Teflon cap containing a glass micro-insert (MACHEREY-NAGEL GmbH & Co.KG).

Samples were analyzed on an Ultimate 3000 UHPLC equipped with an Acclaim column (150 mm × 2.1 mm, particle size 2.2 µm) connected to an IMPACT II UHR-Q-TOF-MS system (Bruker Daltonics, <http://www.bruker.com>). The flow was set to 0.4 mL/min with a solvent gradient decreasing from 90% to 10% of solvent A (water, 0.1% [v/v] acetonitrile and 0.05% formic acid) and increasing from 10% to 90% of solvent B (acetonitrile and 0.05% formic acid) over 20 min after an initial hold of 1 min, followed by column equilibration at starting conditions for 4 min. The MS settings were as follows: end plate offset 500V, capillary 4500V, drying gas 10 L/min at 200 °C, detecting mass range 50-2000 Da, spectra rate 5 Hz. Mass detection was calibrated using sodium formate clusters (v:v, 10 mM NaOH: isopropanol/water containing 0.2% formic acid=

50:50%). Raw data files were analyzed using Bruker Compass DataAnalysis software version 4.3.

#### Caterpillar growth assay

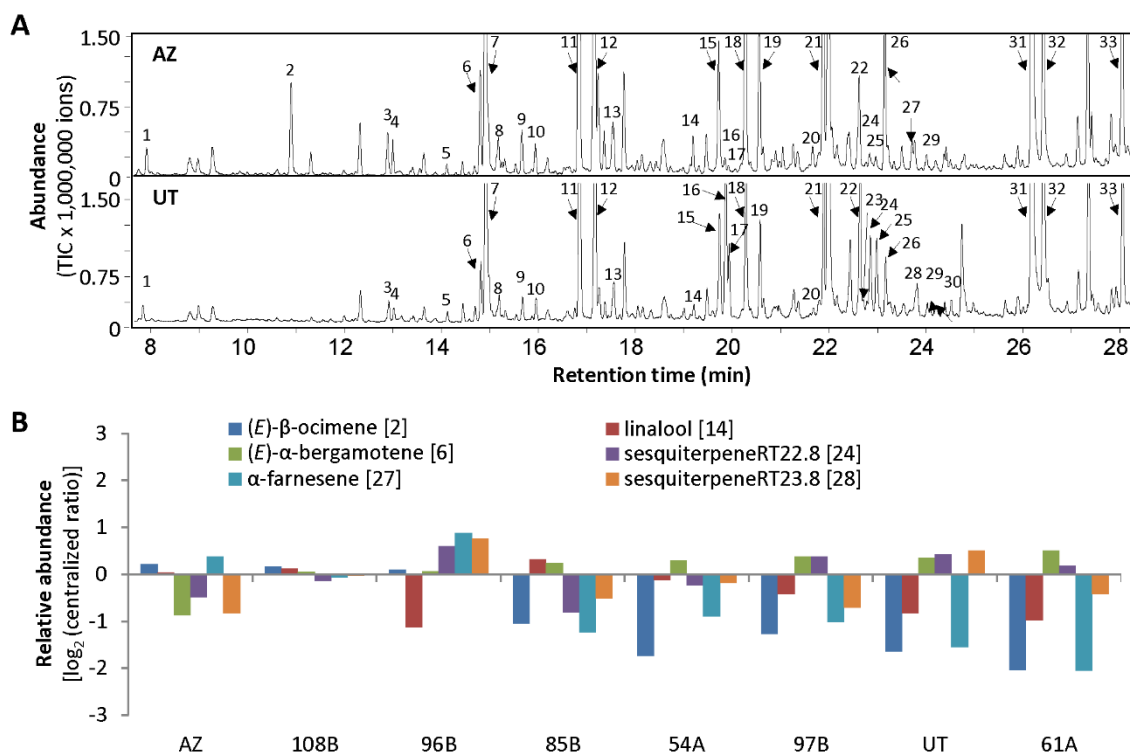
For growth assays on detached leaves, the youngest fully expanded leaf [position +1, (15)] was excised at the base of the petiole and placed into a plastic cup (ca. 650 mL) with wet tissues at the bottom. One first-instar caterpillar was placed on the leaf and kept there for 5 days, at which time the mass of individual caterpillars was measured using a Sartorius BP analytical balance (precision: 0.1 mg, resolution: 0.1 mg, linearity: 0.2 mg, Sartorius Lab Instruments GmbH & Co. KG).

#### Statistical analyses

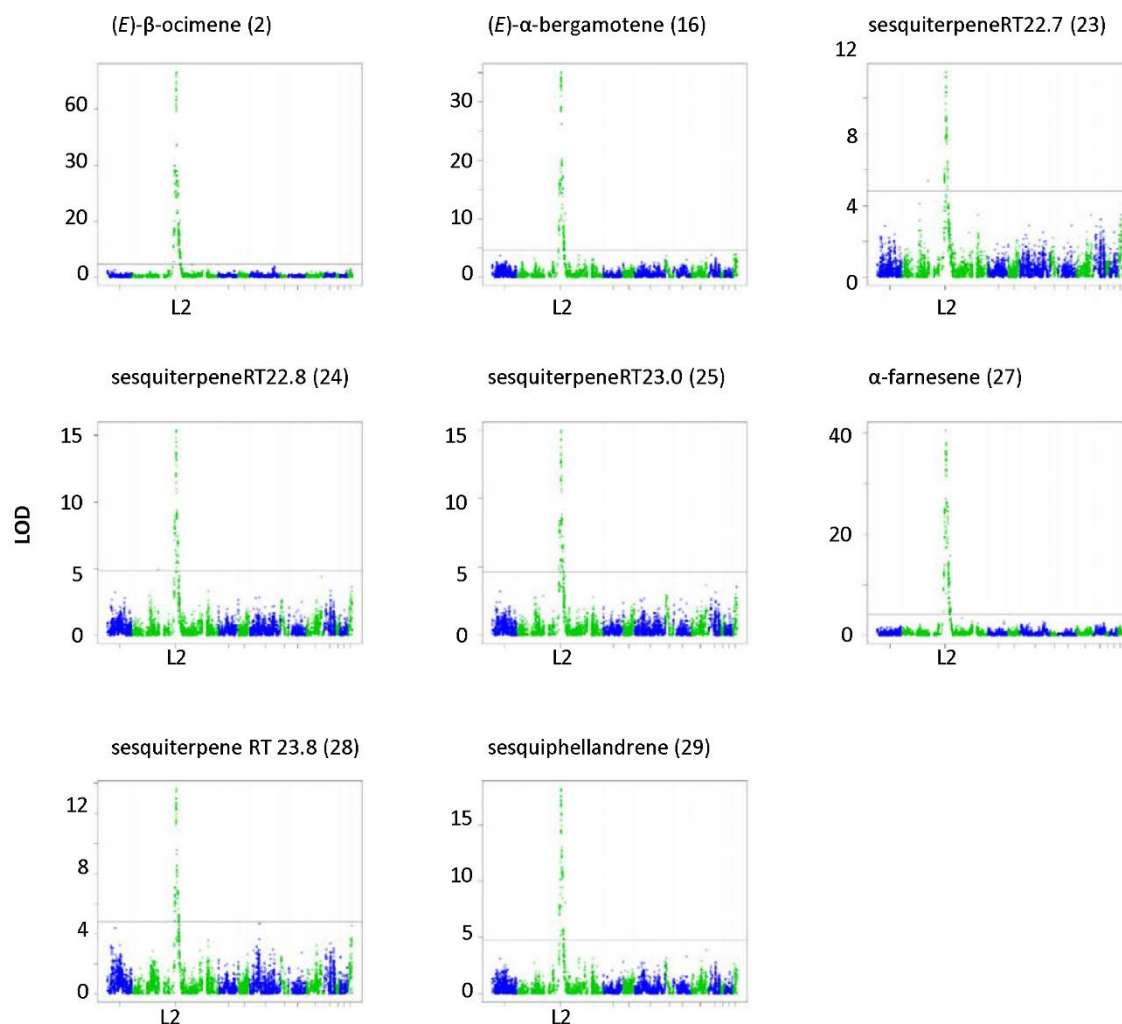
F-tests were used to compare volatile compounds in the headspace of AZ and UT plants, and Bonferroni corrections were used for multiple testing,  $n=5$ . Pearson's correlations were calculated for terpenoid emission versus predation rate; gene expression of *NaLIS*, *NaGPPS1*, 2 versus emission of linalool; and headspace linalool versus glucosidase-released linalool in accessions. Student's *t*-tests were used to compare the relative abundance of *NaLIS* transcripts or linalool emission between VIGS *NaLIS* and VIGS EV plants,  $n=10$ , and the mass of *M. sexta* larvae fed on AZ and ectopic expression lines of AZ background,  $n=20$ . PCA analysis of the relative abundance of terpenoids other than linalool emitted by ectopic expression lines was conducted with ClustVis on centralized data (40). Sign tests were used to compare numbers of touches or eggs received by plants of different genotypes in the wind tunnel or the oviposition chamber. The number of eggs received by each plant in the oviposition chamber was transformed to the proportion of all the eggs laid during the night,  $n=20$ . Friedman tests were used to compare the number of eggs received by plants of six genotypes in the tent assay,  $n=12$ , followed by Tukey-Kramer Multiple Comparisons tests for pairwise comparisons of interest.

Regression and Student's *t*-tests were performed in MS Excel. Sign tests were performed in SPSS Statistics 17.0 (<https://www.ibm.com/analytics/spss-statistics-software>). Friedman test and Tukey-Kramer Multiple Comparisons tests were performed in GraphPad InStat (<https://www.graphpad.com/>). The significance level was set at  $p<0.05$ .

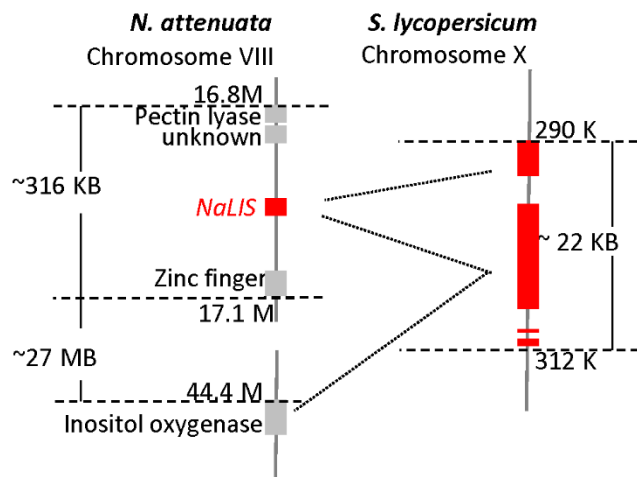




**Fig. S1.** Variation of terpenoids between AZ and UT, and within an AI-RIL population from crossing AZ and UT. A. Representative chromatograms of volatile compounds in headspace of AZ and UT leaves (see Table S1 for compound IDs). B. RILs having different compositions of six terpenoid volatiles, selected for the field predation assay shown in Fig. 1.

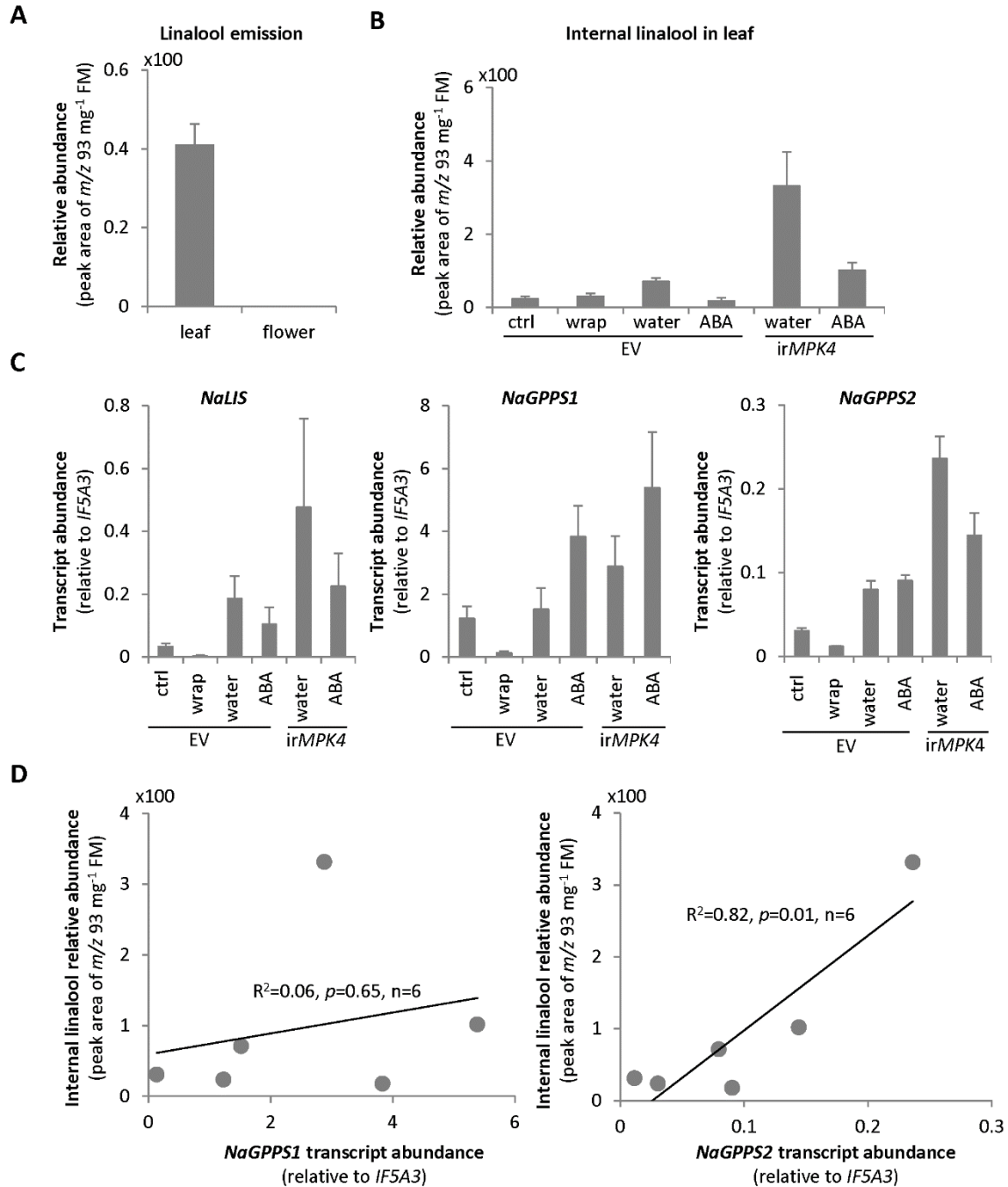


**Fig. S2.** Mapped loci for individual herbivory-induced terpenes using 261 RIL lines. Most terpenes are mapped to a similar locus on linkage group 3 (on chromosome II).



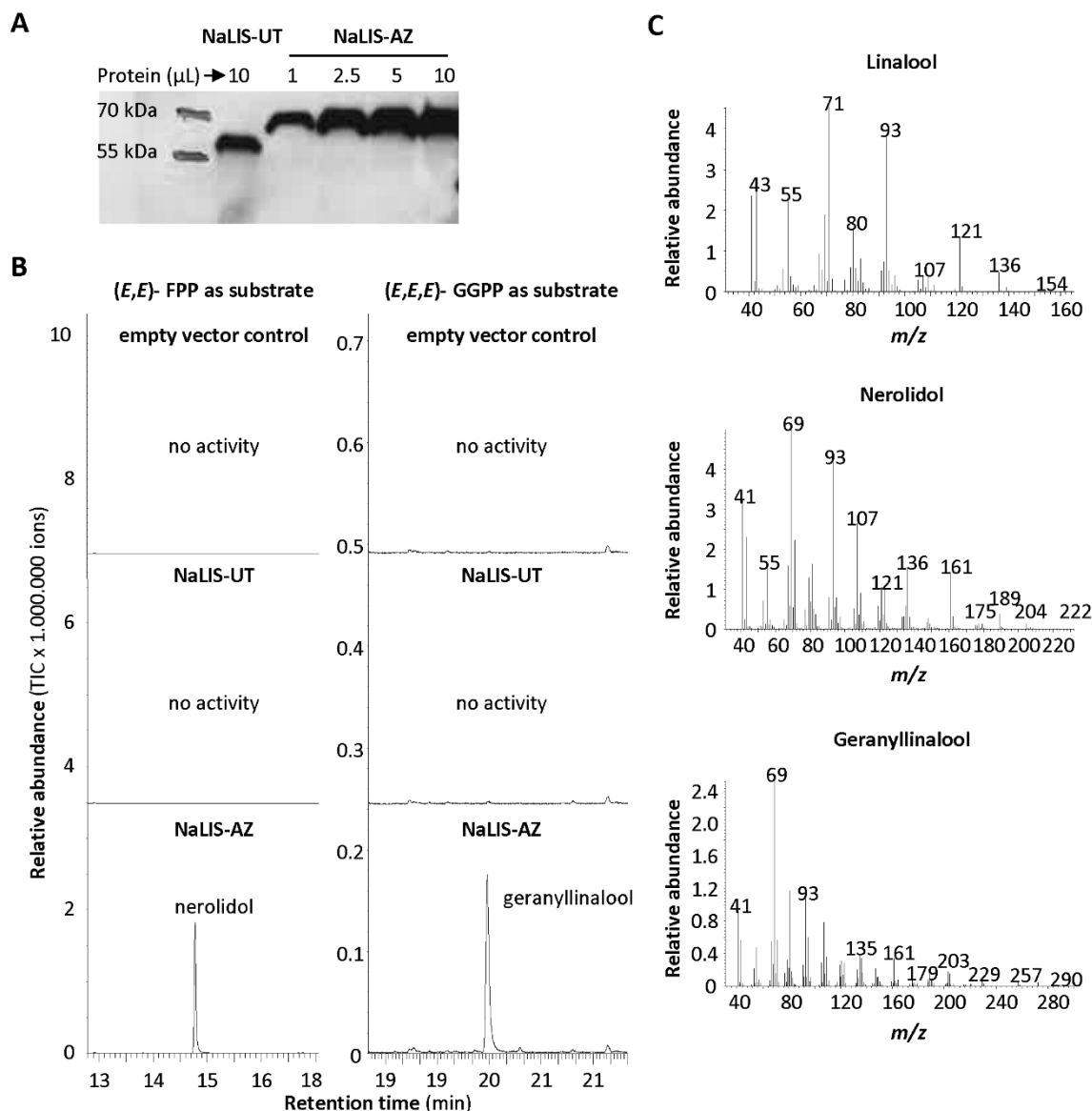
**Fig. S3.** A single *NaTPS* was found within the mapped locus associated with linalool, whereas the homologous region of the tomato genome contained a small cluster of *SlTPS*s. Putative *TPS* genes are shown as red bars, non-*TPS* genes in grey.



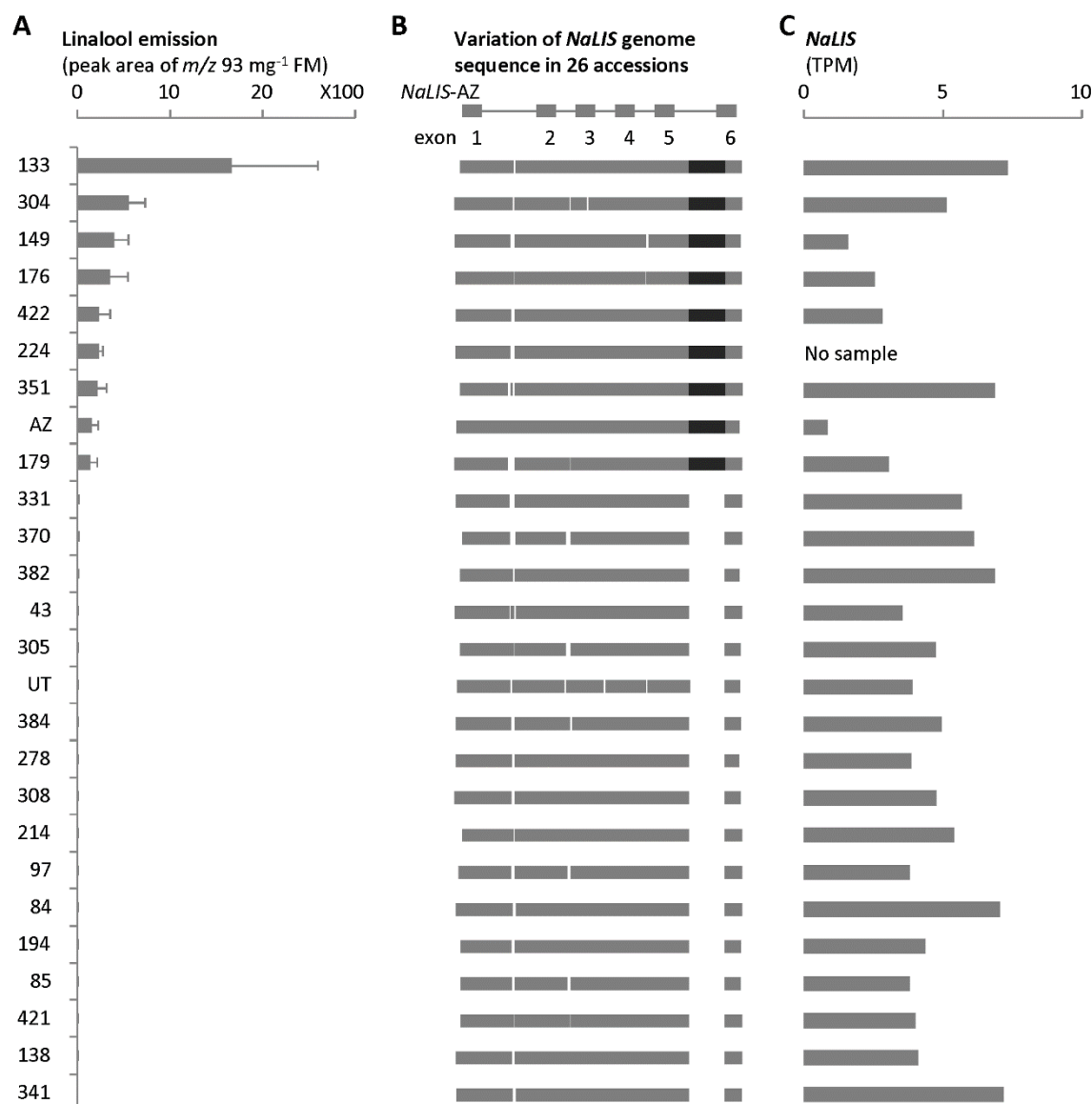


**Fig. S5. Linalool was only detected in the leaf headspace but not in the floral volatiles of UT, and in leaves, the abundance of internal free linalool was correlated with the transcript levels of *NaLIS*, *NaGPPS2* but not *NaGPPS1*.** A. Linalool emitted by leaves or flowers of UT plants (mean+SE,  $n=3$ ). Volatile collection time: 12 hours, from 8:00 to 20:00. B. Abundance of internal free linalool in leaves of EV and transgenic UT (*irMPK4*, a high volatile emitter) plants under different treatments (mean+SE,  $n=3$ ); ctrl: control; wrap: wrapping; ABA: abscisic acid. C. Relative transcript abundance of *NaLIS*, *NaGPPS1* and *NaGPPS2* in same samples as in B (mean+SE,  $n=3$ ). D.

Correlation between the compound in B and the gene transcript level in C. FM: fresh mass.

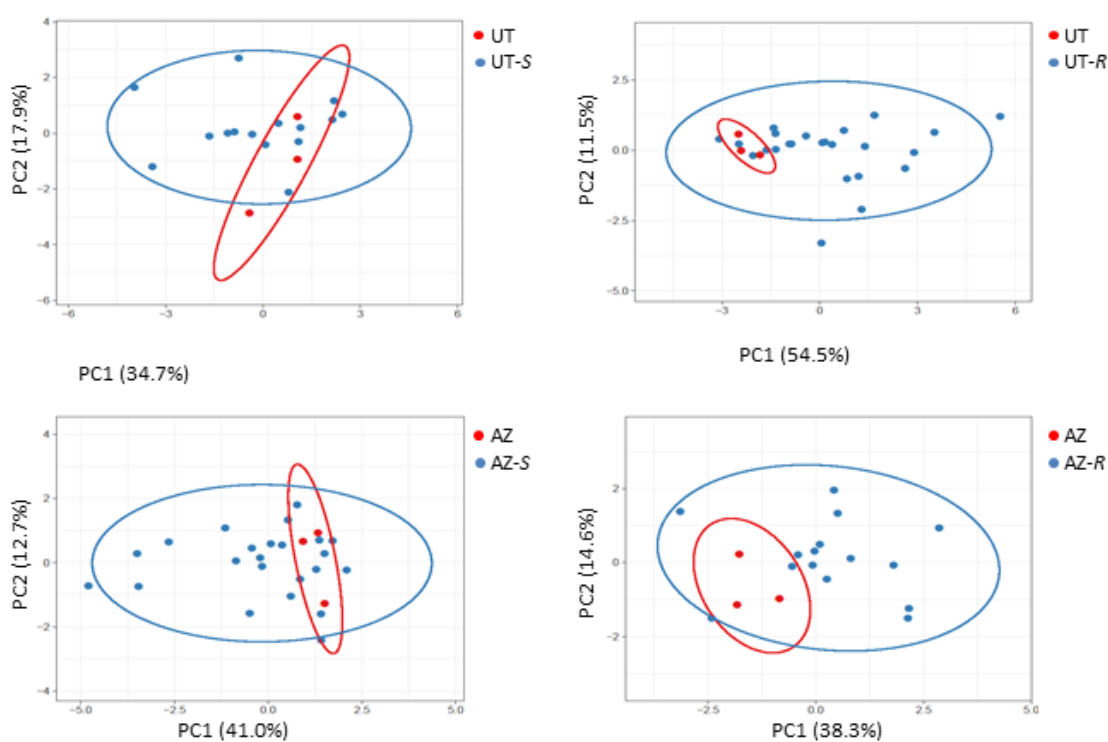


**Fig. S6.** Biochemical characterization of recombinant NaLIS. The alleles were expressed as full-length versions or as N-terminal truncated versions lacking the putative signal peptide in *Escherichia coli*. Shown are data from the truncated proteins; the full-length proteins had lower activity when expressed in *E. coli*. A. Western blot analysis of His-tagged fusion protein of NaLIS-UT and NaLIS-AZ heterologously produced in *E. coli*. The amount of the NaLIS enzymes in *E. coli* raw protein extracts was analyzed using an anti-His-antibody. Different volumes of NaLIS-AZ were compared to 10 μL NaLIS-UT. Similar amount of NaLIS enzymes (10 μL NaLIS-UT extract and 1 μL NaLIS-AZ extract) were used for later assays in B. B. Products by empty vector and recombinant NaLIS alleles from substrate (E,E)-FPP (left) and (E,E,E)-GGPP (right). Product from GPP is shown in Fig. 2F C. Mass spectra of major identified enzyme products.

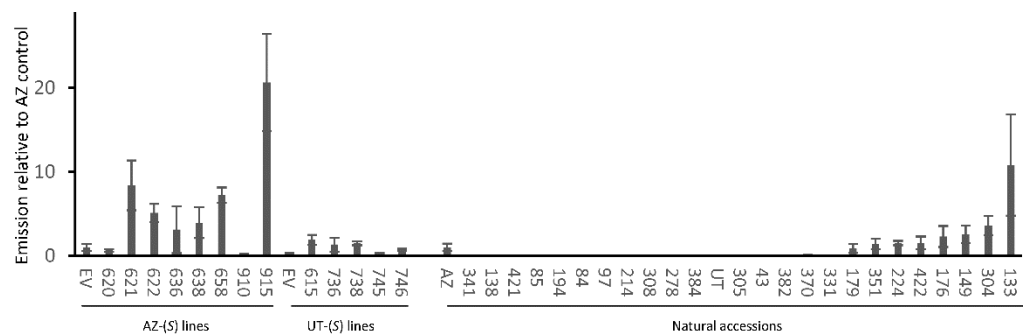


**Fig. S7.** Linalool natural variation correlates with *NaLIS* allelic diversity in 26 *N. attenuata* accessions, but not with the transcript abundance of *NaLIS*. A. Leaf linalool emission after wounding plus *M. sexta* regurgitant treatment (mean+SE, n=3). B. *NaLIS* allele diversity revealed by genome resequencing. Black bars on the top show the structure of *NaLIS* ORF. Grey bars represent genomic sequences (Supplemental File S1) of *NaLIS* in different accessions. Darker grey bars indicate the sequence present in *NaLIS*-AZ variants but missing in *NaLIS*-UT variants. C. Transcript abundance of *NaLIS* in leaves after wounding plus *M. sexta* regurgitant treatment, from RNA-seq data. TPM: transcripts per million.

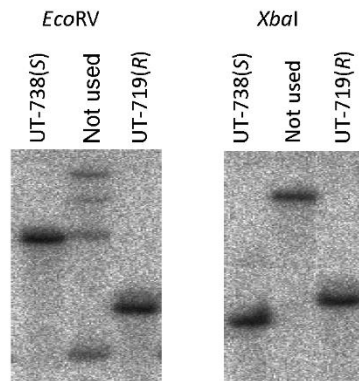
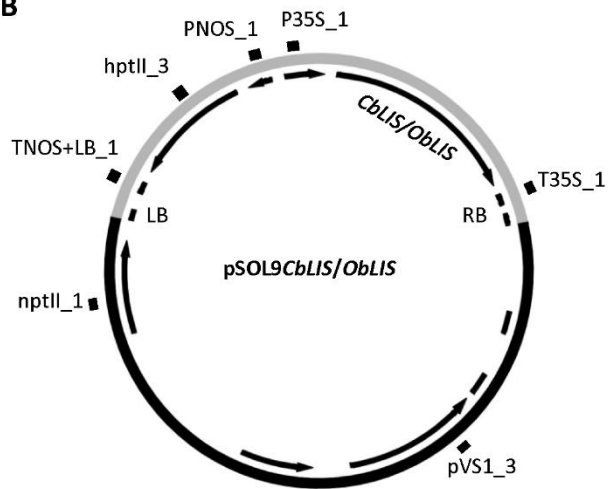
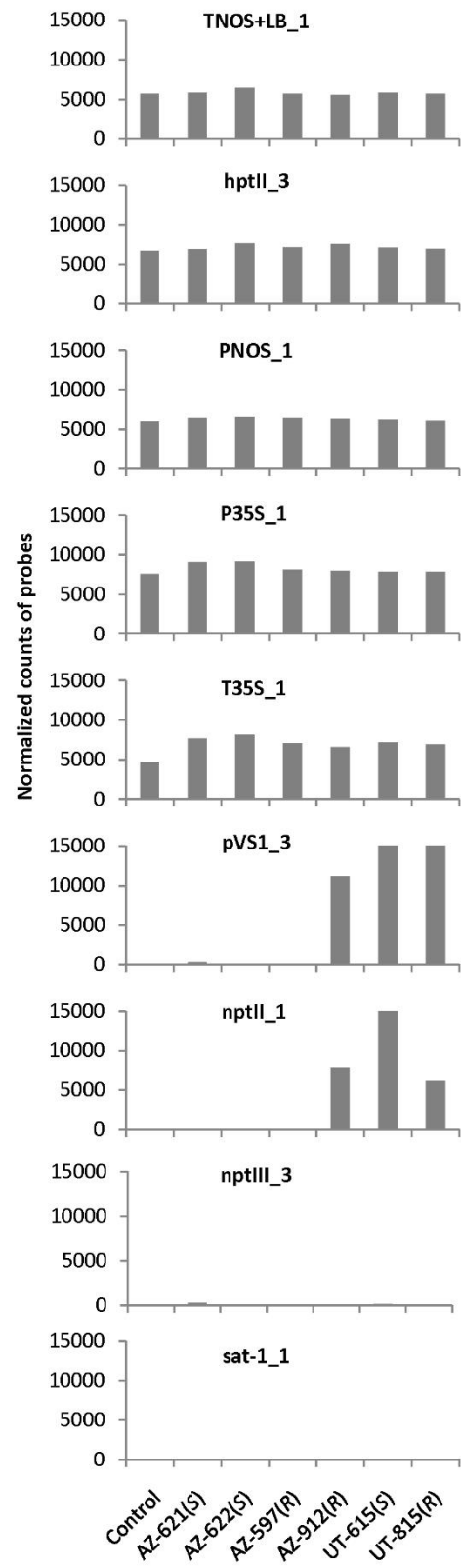




**Fig. S8.** Terpenoid volatiles other than linalool are similar to WT in ectopic expression lines. Shown here are PCAs with 95% confident intervals based on all other detected foliar terpenoid volatiles for ectopic expression lines of each background-transgene combination and responsive WT plants. Input data are in Supplemental File S2.



**Fig. S9.** Normalized linalool emission in ectopic expression lines and natural accessions. Ectopic expression plants and natural accessions were measured in different batches of plants containing AZ and UT EV (empty vector) or WT plants as control for each batch. Emission of linalool was normalized to AZ control plants in each experiment. Ectopic expression lines used for further experiments were 621, 622, 615, and 738.

**A****B****C**

**Fig. S10.** Confirmation of single and complete T-DNA insertions in ectopic expression lines using Southern blotting or Nanostring nCounter® technology. A. Southern blotting with a probe for the hygromycin resistance marker gene HPTII for UT-738(*S*), UT-719(*R*) and an unused line (middle lane) following digestion of genomic DNA with either *Eco*R1 or *Xba*I. B. The map of the pSOL9 plasmid used for transformation. The location of the probes (sequences in Supplemental File S1) used for nCounter analysis are shown as black bars outside the circle. TNOS+LB\_1, hptII\_3, hptII\_3, PNOS\_1, P35S\_1 and T35S\_1 are used to demonstrate single and complete T-DNA insertions. pVS1\_3 and nptII\_1 are probes indicating overreads of the plasmid sequences outside of the T-DNA borders, which do not affect the plant phenotype or its stable inheritance, but may be mentioned when applying for field releases of transgenic plants. C. Counts of hybridized probes to the sheared genomic DNA of independent ectopic expression lines; nptIII\_3 and sat-1\_1 are probes with a sequence not present on the plasmid used as a negative control. The positive control (“Control”) is a line known to contain a single complete insertion without overreads.

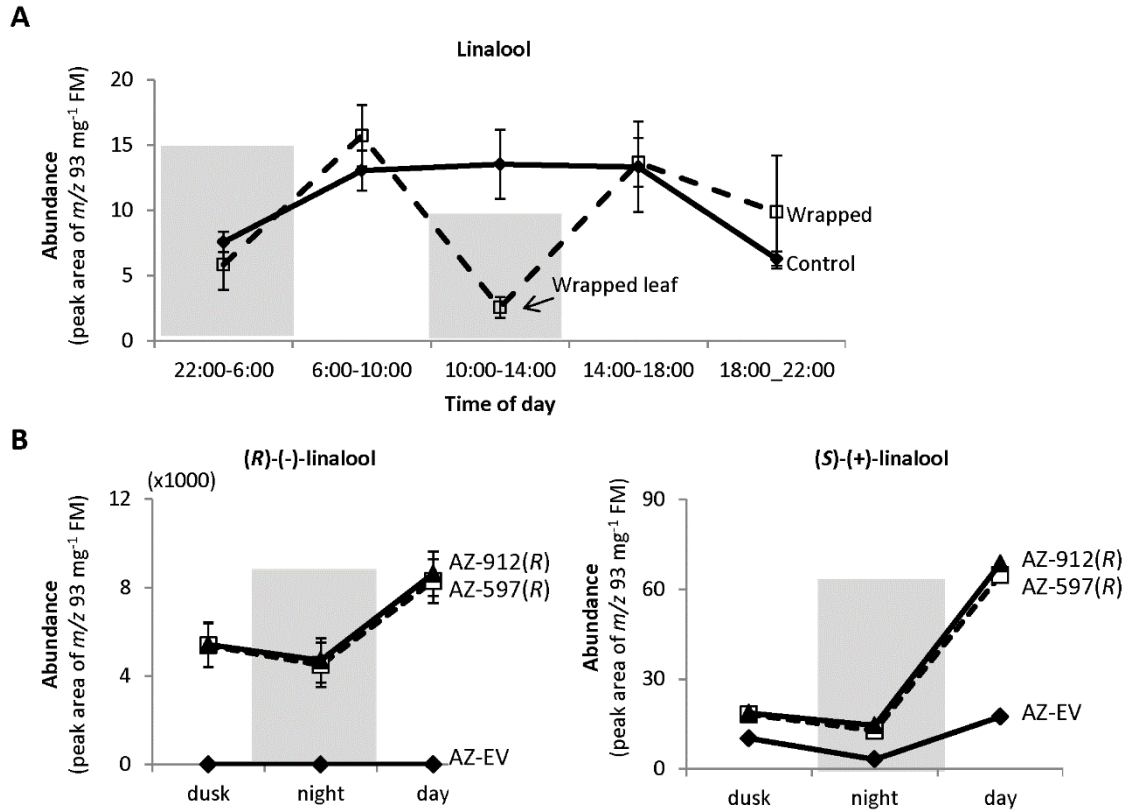


**Fig. S11.** Both ectopically expressed and endogenous linalool emission have a diurnal rhythm and the emission is directly regulated by the presence/absence of light. A: Light deprivation during the middle of the day decreased the emission of linalool in UT plants (mean+SE,  $n=3$ ). Dark periods are indicated by grey bars. B: The emission of the foreign enantiomer, (R)-(-)-linalool and endogenous enantiomer, (S)-(+)-linalool in the transgenic lines in dusk (18:00-22:00), night (22:00-6:00) and day (10:00-18:00). mean+SE,  $n=3$ . FM: fresh mass.

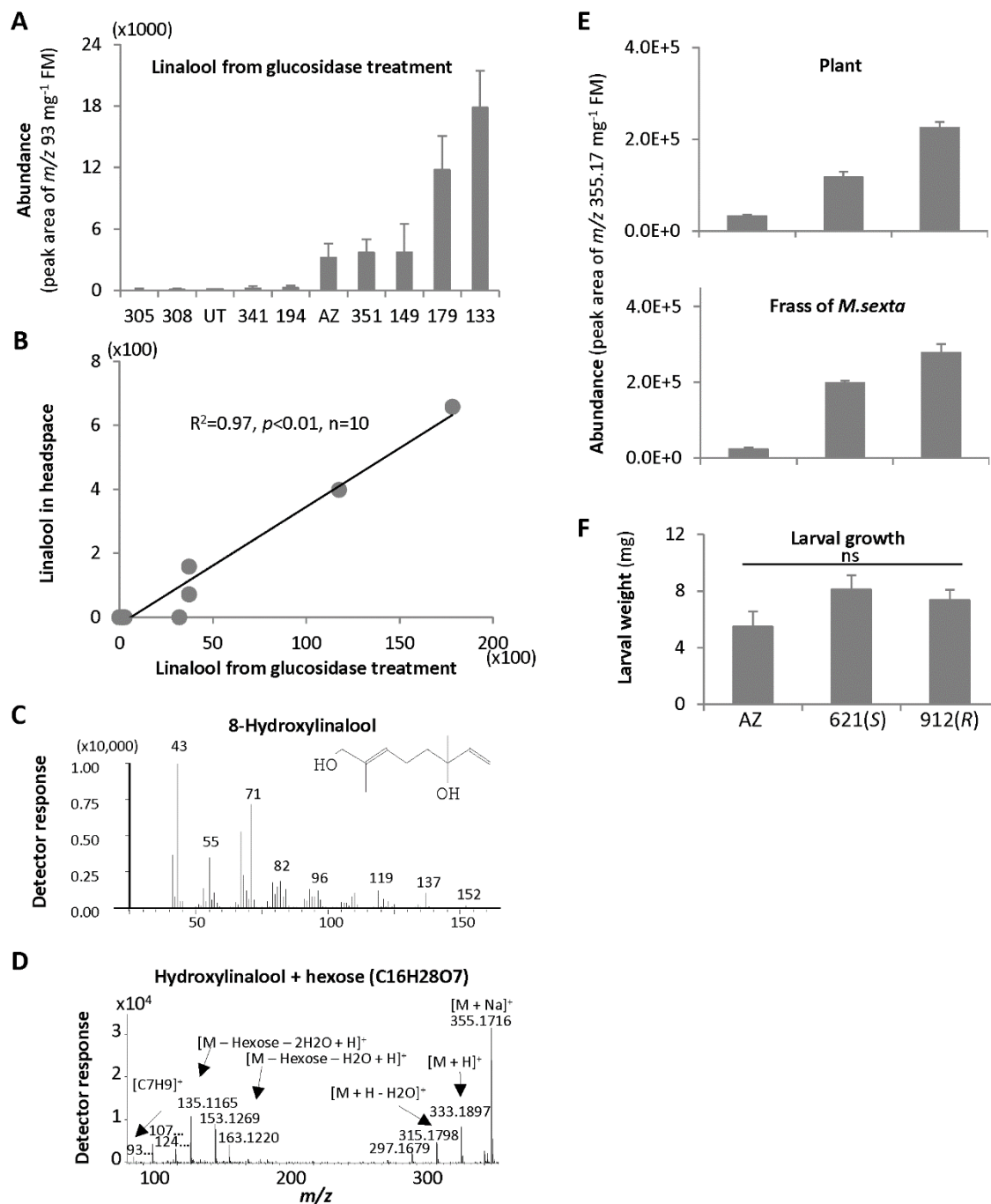


**Fig. S12.** Oxidation/Conjugation of linalool does not regulate the natural variation of linalool emission of *N. attenuata*. **A.** Glucosidase treatment released an abundance of linalool from leaves of *N. attenuata* natural accessions (mean+SE,  $n=3$ ). **B.** Glucosidase-released linalool is strongly correlated with linalool in headspace across the natural accessions. **C.** Hydroxylinalool was also detected in glucosidase-treated leaf material using GC-MS. **D.** Hydroxylinalool conjugates in leaves were detected using UPLC-MS/MS. **E.** Ectopic expression of foreign *LIS* genes increased content of linalool in

leaves (mean+SE, n=3). F. Enhanced linalool enantiomers and conjugates did not affect the growth of *M. sexta* larvae. ns: not significant.

**Table S1.** List of peaks integrated in headspace samples from W+R treated leaves of plants from an AI-RIL population, and mean ( $\pm$ SE) peak areas in the “AZ” and “UT” parental lines. Numbers in bold indicate statistically significant differences between accessions (Bonferroni-corrected  $p < 0.01$  following an F-test).

Index	Name	Retention Time	Target $m/z$	Reference $m/z$	AZ (Peak area $\times 10^5$ )	UT (Peak area $\times 10^5$ )
1	1-hexanal	7.75	56	41	0.42 $\pm$ 0.06	0.45 $\pm$ 0.06
2	( <i>E</i> )- $\beta$ -ocimene	10.90	93		<b>4.44<math>\pm</math>0.84</b>	<b>0.13<math>\pm</math>0.01</b>
3	( <i>Z</i> )-3-hexen-1-ol-acetate	12.95	67	82.1	2.84 $\pm$ 0.77	1.29 $\pm$ 0.24
4	unknown GLV	13.01	56		0.92 $\pm$ 0.28	1.39 $\pm$ 0.21
5	1-hexanol	14.16	56	69	0.93 $\pm$ 0.18	1.20 $\pm$ 0.28
6	( <i>Z</i> )-3-hexenyl propanoate	14.80	67	57; 82	5.07 $\pm$ 1.16	4.85 $\pm$ 0.66
7	( <i>Z</i> )-3-hexenyl butanoate	14.91	67	55; 82	25.5 $\pm$ 5.25	30.9 $\pm$ 5.76
8	( <i>E</i> )-2-hexenyl butanoate	15.17	71	43	1.39 $\pm$ 0.29	2.53 $\pm$ 0.45
9	n-hexyl butanoate	15.66	71	56	1.14 $\pm$ 0.34	1.52 $\pm$ 0.38
10	hexyl-2-methyl butanoate	15.94	57	85; 103	0.59 $\pm$ 0.18	1.21 $\pm$ 0.23
11	( <i>E</i> )-3-hexenyl butanoate	16.90	67	82; 55	48.2 $\pm$ 12.7	40.5 $\pm$ 8.90
12	( <i>Z</i> )-3-hexenyl valerate	17.15	67	82; 57	44.5 $\pm$ 12.0	40.5 $\pm$ 6.03
13	( <i>Z</i> )-3-hexenyl isovalerate	17.53	67	82	1.55 $\pm$ 0.27	2.17 $\pm$ 0.19
14	linalool	19.19	93		<b>0.56<math>\pm</math>0.09</b>	<b>0.16<math>\pm</math>0.02</b>
15	$\alpha$ -duprezianene	19.78	119	161; 91	2.39 $\pm$ 0.29	2.98 $\pm$ 0.57
16	( <i>E</i> )- $\alpha$ -bergamotene	19.85	119	107	<b>0.35<math>\pm</math>0.06</b>	<b>13.4<math>\pm</math>3.37</b>
17	$\beta$ -elemene	19.92	147	189	<b>0.01<math>\pm</math>0.00</b>	<b>0.68<math>\pm</math>0.21</b>
18	( <i>Z</i> )-3-hexenyl caproate	20.34	82	67; 99	16.5 $\pm$ 3.31	20.7 $\pm$ 4.09
19	unknown GLV	20.56	82	67; 99	5.65 $\pm$ 1.79	8.55 $\pm$ 1.81
20	( <i>Z</i> )-3-hexenyl hexanoate	21.66	67	82; 141	0.61 $\pm$ 0.13	0.55 $\pm$ 0.08
21	unknown GLV	21.87	67	82; 55	12.2 $\pm$ 2.91	19.7 $\pm$ 3.63
22	$\alpha$ -terpineol	22.62	93	121; 136	<b>2.00<math>\pm</math>0.31</b>	<b>6.43<math>\pm</math>1.18</b>
23	sesquiterpeneRT22.7	22.68	161	147	<b>0.02<math>\pm</math>0.00</b>	<b>0.25<math>\pm</math>0.05</b>
24	sesquiterpeneRT22.8	22.83	93	121	<b>0.10<math>\pm</math>0.03</b>	<b>1.66<math>\pm</math>0.34</b>
25	sesquiterpeneRT23.0	22.96	93	189; 133	<b>0.06<math>\pm</math>0.02</b>	<b>1.89<math>\pm</math>0.45</b>
26	unknown GLV	23.15	67	55; 82	4.42 $\pm$ 1.35	4.35 $\pm$ 0.94
27	$\alpha$ -farnesene	23.71	93	107	<b>0.48<math>\pm</math>0.12</b>	<b>0.01<math>\pm</math>0.00</b>
28	sesquiterpeneRT23.8	23.80	93	147	<b>0.02<math>\pm</math>0.00</b>	<b>0.76<math>\pm</math>0.20</b>
29	sesquiphellandrene	24.07	93	161	<b>0.03<math>\pm</math>0.01</b>	<b>0.21<math>\pm</math>0.04</b>
30	sesquiterpeneRT24.2	24.24	93	119	<b>0.05<math>\pm</math>0.01</b>	<b>0.26<math>\pm</math>0.03</b>
31	nicotine	26.18	84	133; 162	<b>67.4<math>\pm</math>16.4</b>	<b>233<math>\pm</math>51.4</b>
32	benzyl alcohol	26.46	79	108; 77	19.0 $\pm$ 0.77	15.3 $\pm$ 1.75
33	sesquiterpeneRT27.3	27.39	121	93	7.31 $\pm$ 0.87	9.54 $\pm$ 1.54



**Table S2.** Transgenic lines used in this study.

Line number	Abbreviation	Background	Trans-gene	Enhanced linalool enantiomer
A-09-620	AZ-620( <i>S</i> )	AZ	<i>CbLIS</i> full ORF [Genbank: CBU58314, (4)]	(S)-(+)-linalool
<b>A-09-621</b>	<b>AZ-621(<i>S</i>)</b>			
<b>A-09-622</b>	<b>AZ-622(<i>S</i>)</b>			
A-09-636	AZ-636( <i>S</i> )			
A-09-638	AZ-638( <i>S</i> )			
A-09-658	AZ-658( <i>S</i> )			
A-09-910	AZ-910( <i>S</i> )			
A-09-915	AZ-915( <i>S</i> )	UT	<i>ObLIS</i> full ORF [GenBank: AY693647, (5)]	(R)-(-)-linalool
<b>A-09-615</b>	<b>UT-615(<i>S</i>)</b>			
A-09-736	UT-736( <i>S</i> )			
<b>A-09-738</b>	<b>UT-738(<i>S</i>)</b>			
A-09-745	UT-745( <i>S</i> )			
A-09-746	UT-746( <i>S</i> )	AZ	<i>Fragments of NaMPK4</i> [GenBank: HQ236013, (9)] <i>in inverted repeat orientation</i>	*
<b>A-09-597</b>	<b>AZ-597(<i>R</i>)</b>			
A-09-625	AZ-625( <i>R</i> )			
A-09-630	AZ-630( <i>R</i> )			
<b>A-09-912</b>	<b>AZ-912(<i>R</i>)</b>			
A-09-946	AZ-946( <i>R</i> )	UT	<i>Fragments of NaMPK4</i> [GenBank: HQ236013, (9)] <i>in inverted repeat orientation</i>	*
A-09-680	UT-680( <i>R</i> )			
<b>A-09-719</b>	<b>UT-719(<i>R</i>)</b>			
A-09-788	UT-788( <i>R</i> )			
A-09-789	UT-789( <i>R</i> )			
<b>A-09-815</b>	<b>UT-815(<i>R</i>)</b>			
A-09-1168	UT-1168( <i>R</i> )			
A-09-1170	UT-1170( <i>R</i> )			
A-09-1174	UT-1174( <i>R</i> )	UT	<i>Fragments of NaMPK4</i> [GenBank: HQ236013, (9)] <i>in inverted repeat orientation</i>	*
A-08-119	irMPK4			

Lines in **bold**: selected for assays of oviposition preference and larval growth. \*This line generally emits more all kinds of *N. attenuata* volatiles than WT plants.

**Table S3.** Primers used for qPCR or PCR amplification in this study.

Experiment	Gene	Primer	
qPCR	<i>NaLIS</i>	Forward	TACATGAGATCACCTTATAGGGCAC
		Reverse	TGCATAGATTTCCCCACGTCT
	<i>NaGPPS1</i>	Forward	CATTGAAATGATCCATACTGCAAGC
		Reverse	CCAGCCAGTACTGCCACTC
	<i>NaGPPS2</i>	Forward	TATGGGAAAAATTTGGGCTTGGC
		Reverse	TGGCATAACAATATAGGGGCAGTT
	<i>IF5A3F</i>	Forward	GTCGGACGAAGAACACCATT
		Reverse	CACATCACAGTTGTGGGAGG
			TAGAACTAGTGGATCTGTGTCGCGGTAGCTAAAG
VIGS	<i>NaLIS</i>	Forward	A
		Reverse	CCCCCTCGAGGTCGAGGAGTGCATGTGCTCTCAGT
Transcript size	<i>NaLIS</i> -UT CDS	Forward	ATGGCAATGACTAGAGCACTCTCC
		Reverse	CTATTGTTCCGTGGCAAATTCAGA
	<i>NaLIS</i> -AZ CDS	Forward	ATGGCAATGACTAGAGCACTCTCC
		Reverse	CTACACATGCAACATAGACTTGATGT
	<i>NaLIS</i> -transcript	Forward	GCACTCTTTACAGATCCAAGAATGT
		Reverse	CTATTGTTCCGTGGCAAATTCAGA
N-terminal truncated	<i>NaLIS</i> -UT	Forward	CACCATTCAGGTTTCATGCGGAAGCTC
		Reverse	CTACACATGCAACATAGACTTGA
	<i>NaLIS</i> -AZ	Forward	CACCATTCAGGTTTCATGCGGAAGCTC
		Reverse	CTATTGTTCCGTGGCAAATTCAGA

## References

1. Glawe GA, Zavala JA, Kessler A, Van Dam NM, & Baldwin IT (2003) Ecological costs and benefits correlated with trypsin protease inhibitor production in *Nicotiana attenuata*. *Ecology* 84(1):79-90.
2. Baldwin IT, Staszakozinski L, & Davidson R (1994) Up in smoke .1. smoke-derived germination cues for postfire annual, *Nicotiana attenuata* Torr ex Watson. *J Chem Ecol* 20(9):2345-2371.
3. Zhou WW, Kügler A, McGale E, Haverkamp A, Knaden M, Guo H, Beran F, Yon F, Li R, Lackus N, Köllner TG, Bing J, Schuman MC, Hansson BS, Kessler D, Baldwin IT, & Xu SQ (2017) Tissue-specific emission of (*E*)- $\alpha$ -bergamotene helps resolve the dilemma when pollinators are also herbivores. *Curr Biol* 27(9):1336-1341.
4. Dudareva N, Cseke L, Blanc VM, & Pichersky E (1996) Evolution of floral scent in *Clarkia*: Novel patterns of S-linalool synthase gene expression in the *C. breweri* flower. *Plant Cell* 8(7):1137-1148.
5. Iijima Y, Davidovich-Rikanati R, Fridman E, Gang DR, Bar E, Lewinsohn E, & Pichersky E (2004) The biochemical and molecular basis for the divergent patterns in the biosynthesis of terpenes and phenylpropenes in the peltate glands of three cultivars of basil. *Plant Physiol* 136(3):3724-3736.
6. Gase K, Weinhold A, Bozorov T, Schuck S, & Baldwin IT (2011) Efficient screening of transgenic plant lines for ecological research. *Mol Ecol Resour* 11(5):890-902.
7. Krügel T, Lim M, Gase K, Halitschke R, & Baldwin IT (2002) Agrobacterium-mediated transformation of *Nicotiana attenuata*, a model ecological expression system. *Chemoecology* 12(4):177-183.
8. Bubner B, Gase K, Berger B, Link D, & Baldwin IT (2006) Occurrence of tetraploidy in *Nicotiana attenuata* plants after *Agrobacterium*-mediated transformation is genotype specific but independent of polysomaty of explant tissue. *Plant Cell Rep* 25(7):668-675.
9. Hettenhausen C, Baldwin IT, & Wu J (2012) Silencing *MPK4* in *Nicotiana attenuata* enhances photosynthesis and seed production but compromises abscisic acid-induced stomatal closure and guard cell-mediated resistance to *Pseudomonas syringae* pv tomato DC3000. *Plant Physiol* 158(2):759-776.
10. Schuman MC, Barthel K, & Baldwin IT (2012) Herbivory-induced volatiles function as defenses increasing fitness of the native plant *Nicotiana attenuata* in nature. *eLife* 1.
11. Kessler D, Kallenbach M, Diezel C, Rothe E, Murdock M, & Baldwin IT (2015) How scent and nectar influence floral antagonists and mutualists. *eLife* 4.
12. McGale E, Diezel C, Schuman MC, & Baldwin IT (2018) Cry1Ac production is costly for native plants attacked by non-Cry1Ac-targeted herbivores in the field. *New Phytol* 219(2):714-727.
13. Halitschke R, Schittko U, Pohnert G, Boland W, & Baldwin IT (2001) Molecular interactions between the specialist herbivore *Manduca sexta* (Lepidoptera, Sphingidae) and its natural host *Nicotiana attenuata*. III. Fatty acid-amino acid conjugates in herbivore oral secretions are necessary and sufficient for herbivore-specific plant responses. *Plant Physiol* 125(2):711-717.
14. Schittko U, Preston CA, & Baldwin IT (2000) Eating the evidence? *Manduca sexta* larvae can not disrupt specific jasmonate induction in *Nicotiana attenuata* by rapid consumption. *Planta* 210(2):343-346.
15. Van Dam NM, Horn M, Mares M, & Baldwin IT (2001) Ontogeny constrains systemic protease inhibitor response in *Nicotiana attenuata*. *J Chem Ecol* 27(3):547-568.
16. Kallenbach M, Oh Y, Eilers EJ, Veit D, Baldwin IT, & Schuman MC (2014) A robust, simple, high-throughput technique for time-resolved plant volatile analysis in field experiments. *Plant J* 78(6):1060-1072.

17. Kallenbach M, Veit D, Eilers EJ, & Schuman MC (2015) Application of silicone tubing for robust, simple, high-throughput, and time-resolved analysis of plant volatiles in field experiments. *Bio Protoc* 5(3).
18. Cheng R, Abney M, Palmer AA, & Skol AD (2011) QTLRel: an R package for genome-wide association studies in which relatedness is a concern. *BMC Genet* 12:66.
19. van Pinxteren M, Paschke A, & Popp P (2010) Silicone rod and silicone tube sorptive extraction. *J Chromatogr A* 1217(16):2589-2598.
20. Matsui K, Sugimoto K, Mano J, Ozawa R, & Takabayashi J (2012) Differential metabolisms of green leaf volatiles in injured and intact parts of a wounded leaf meet distinct ecophysiological requirements. *Plos One* 7(4).
21. Lückner J, Bouwmeester HJ, Schwab W, Blaas J, van der Plas LH, & Verhoeven HA (2001) Expression of *Clarkia* S-linalool synthase in transgenic petunia plants results in the accumulation of S-linalyl- $\beta$ -D-glucopyranoside. *Plant J* 27(4):315-324.
22. Brockmoller T, Ling ZH, Li DP, Gaquerel E, Baldwin IT, & Xu SQ (2017) *Nicotiana attenuata* Data Hub (NaDH): an integrative platform for exploring genomic, transcriptomic and metabolomic data in wild tobacco. *BMC Genet* 18.
23. Xu SQ, Brockmoller T, Navarro-Quezada A, Kuhl H, Gase K, Ling ZH, Zhou WW, Kreitzer C, Stanke M, Tang HB, Lyons E, Pandey P, Pandey SP, Timmermann B, Gaquerel E, & Baldwin IT (2017) Wild tobacco genomes reveal the evolution of nicotine biosynthesis. *Proc Natl Acad Sci U S A* 114(23):6133-6138.
24. Li H & Durbin R (2009) Fast and accurate short read alignment with Burrows-Wheeler transform. *Bioinformatics* 25(14):1754-1760.
25. Holt C & Yandell M (2011) MAKER2: an annotation pipeline and genome-database management tool for second-generation genome projects. *BMC Bioinformatics* 12:491.
26. Stanke M, Keller O, Gunduz I, Hayes A, Waack S, & Morgenstern B (2006) AUGUSTUS: ab initio prediction of alternative transcripts. *Nucleic Acids Res* 34(Web Server issue):W435-W239.
27. Korf I (2004) Gene finding in novel genomes. *BMC Bioinformatics* 5:59.
28. Lomsadze A, Ter-Hovhannisyan V, Chernoff YO, & Borodovsky M (2005) Gene identification in novel eukaryotic genomes by self-training algorithm. *Nucleic Acids Res* 33(20):6494-6506.
29. Bray NL, Pimentel H, Melsted P, & Pachter L (2016) Near-optimal probabilistic RNA-seq quantification. *Nat Biotechnol* 34(5):525-527.
30. Quinlan AR & Hall IM (2010) BEDTools: a flexible suite of utilities for comparing genomic features. *Bioinformatics* 26(6):841-842.
31. Thorvaldsdottir H, Robinson JT, & Mesirov JP (2013) Integrative Genomics Viewer (IGV): high-performance genomics data visualization and exploration. *Brief Bioinform* 14(2):178-192.
32. Galis I, Schuman MC, Gase K, Hettenhausen C, Hartl M, Dinh ST, Wu J, Bonaventure G, & Baldwin IT (2013) The use of VIGS technology to study plant-herbivore interactions. *Methods Mol Biol* 975:109-137.
33. Krügel T, Lim M, Gase K, Halitschke R, & Baldwin IT (2002) Agrobacterium-mediated transformation of *Nicotiana attenuata*, a model ecological expression system. *Chemoecology* 12(4):177-183.
34. Zavala JA, Patankar AG, Gase K, & Baldwin IT (2004) Constitutive and inducible trypsin proteinase inhibitor production incurs large fitness costs in *Nicotiana attenuata*. *Proceedings of the National Academy of Sciences of the United States of America* 101(6):1607-1612.
35. Bubner B, Gase K, Berger B, Link D, & Baldwin IT (2006) Occurrence of tetraploidy in *Nicotiana attenuata* plants after *Agrobacterium*-mediated transformation is genotype specific but independent of polysomaty of explant tissue. *Plant cell reports* 25(7):668-675.

36. Gase K & Baldwin IT (2012) Transformational tools for next-generation plant ecology: manipulation of gene expression for the functional analysis of genes. *Plant Ecol Divers* 5(4):485-490.
37. Schäfer M, *et al.* (2013) 'Real time' genetic manipulation: a new tool for ecological field studies. *The Plant journal : for cell and molecular biology* 76(3):506-518.
38. Bell RA & Joachim FG (1976) Techniques for rearing laboratory colonies of tobacco hornworms and pink bollworms. *Ann Entomol Soc Am* 69(2):365-373.
39. Haverkamp A, Bing J, Badeke E, Hansson BS, & Knaden M (2016) Innate olfactory preferences for flowers matching proboscis length ensure optimal energy gain in a hawkmoth. *Nat Comm* 7:11644.
40. Metsalu T & Vilo J (2015) ClustVis: a web tool for visualizing clustering of multivariate data using Principal Component Analysis and heatmap. *Nucleic Acids Res* 43(W1):W566-W570.